# Journal of Applied Sciences

ISSN 1812-5654

Journal of Applied Sciences 12 (19): 2044-2051, 2012
ISSN 1812-5654 / DOI: 10.3923/jas.2012.2044.2051


# Temporal Change Monitoring of Mangrove Distribution in Penang Island from 2002-2010 by Remote Sensing Approach

B.C. Beh, M.Z. MatJafri and H.S. Lim
School of Physics, Universiti Sains Malaysia, 11800 Penang, Malaysia

**Abstract:** Environmental study is vital for the purpose of monitoring and management of ecological status of mangrove ecosystem. Due to the difficulty to access and penetrate into the mangrove area along the coastal region, assessment of the mangrove can be studied by using remote sensing technique. In this study, the former and current condition of mangrove distribution in Penang Island, Malaysia was mapped by using Landsat-7 ETM+ and THEOS imagery. The two sets of data will be processed using supervised classification method, Maximum Likelihood Classifier in PCI Geomatica version 10.3.2 digital image processing software. The location of each mangrove sample was recorded using handheld global positioning systems during field survey to the study site. The *in situ* data was then being analyzed in laboratory and the actual location of mangrove area was registered into the Thailand Earth Observation System (THEOS) data to generate a geocoded map showing on distribution of mangrove over Penang Island on 2010. Confusion (error) matrix and kappa coefficient were computed to determine the agreement between the classified and reference data. The higher accuracy results of 94.40% for THEOS data and 94.00%for Landsat data indicate that the two sets of data can be used effectively to discriminate the mangrove area and monitor the mangrove changes in Penang Island. In the 8 years (2002-2008) period, mangrove cover over Penang Island had experienced an increment with area change of 12.30%.

**Key words:** Mangrove, Thailand earth observing system, Malaysia, maximum likelihood classifier, PCI geomatica

## INTRODUCTION

Mangrove is a salt tolerant species of woody plants that can be found in tropical and subtropical climate country along sheltered coastal area and intertidal zones (Jensen *et al*., 2007). They can live in high salinity soil and brackish water condition with their special prop root systems (pneumatophores). Mangrove trees not only provide food to marine life and its associated community but also serve as natural barrier to protect the inland area or shoreline from storms, floods, erosion or tsunami (Liu *et al*., 2007). Beside, mangrove forestry products such as firewood, charcoal and timber contributes a lot of profit to their country's income. Therefore, mangrove plays a vital role in the flora and fauna ecosystem and has very important environmental, ecological, biological and economic values (Mitsch *et al*., 2002).

In order to have an effective monitoring of mangrove changes over time, accurate, rapid and cost effective mapping techniques is necessary (Green *et al*., 1998; Liu *et al*., 2007) as the conventional technique to monitor the mangrove area is time-consuming, expensive and labor-intensive (Lee and Yeh, 2009). The use of remotely sensed data and technology is capable to offer many advantages in many areas such as deforestation monitoring, water quality and geology mapping, land surface temperature retrieval and long-term environmental changes management (Green *et al*., 1996; Coulibaly and Goita, 2006; Tan *et al*., 2010).

Currently the uncontrolled deforestation of mangrove forest into aquaculture or urban area has lead to the serious declining in mangrove forest. Prior to 1990, Malaysia had lost almost 30% of mangroves forest and the declining rate is expected to continue at a rate of 1% per year (Gong and Ong, 1990). In order to monitor and preserve the mangrove ecosystem efficiently, different remote sensing technique has been utilized and invented by researchers to extract the mangrove information from high resolution satellite data or hyperspectral data (Jensen *et al*., 2007).

Application of remote sensing technique on mangrove mapping in Malaysia is limited. Some of the research which had been done in Malaysia include the analysis of Landsat TM imagery and different scale of aerial photographs has successful distinguish 7 and 14 mangrove forest types, respectively in Kemaman District,

**Corresponding Author:** B.C. Beh, School of Physics, Universiti Sains Malaysia, 11800 Penang, Malaysia
Tel: +604-6533888 Fax: +604-6579150

Terengganu, Malaysia (Sulong *et al*., 2002). In recent work, Ibrahim *et al*. (2010) had used four types of vegetation indices namely Global Environmental Monitoring Index (GEMI), Atmospherically Resistant Vegetation Index (ARVI), Modified Aerosol Free Vegetation Index Mid-Infrared (Modified AFRI MIR) and Modified Aerosol Free Vegetation Index Shortwave Infra-red (Modified AFRI SWIR) derived from Landsat-5 TM for mangrove mapping at Kelantan Delta. In Sabah State, Malaysia, ALOS Advanced Visible and Near Infrared Radiometer type-2 (AVNIR-2), ALOS Panchromatic Remote-sensing Instrument for Stereo Mapping (PRISM), Landsat TM and JERS Very Near Infrared Radiometer type-1 (VNIR-1) imagery were also used for monitoring the changes in mangrove cover in Tawau Merotai and Tuaran area (Polpanich *et al*., 2009).

Normalized Difference Vegetation Index (NDVI) analysis was a popular method used for monitoring of green vegetation. A study had used five different remote sensing approaches which are visual interpretation, supervised classification, unsupervised classification, NDVI image and band ratios on Landsat TM, SPOT XS and CASI data to classify the mangrove and non-mangrove vegetations in Turks and Caicos Island (Green *et al*., 1998). In addition, based on the study by Emch and Peterson (2006), Maximum Likelihood Classification (MLC), NDVI image and subpixel classification were used to compare the temporal changes of mangrove forest in the Sundarbans of southwest Bangladesh from 1989-2000. Furthermore, discrimination of mangrove distribution in Danshui River estuary in Taipei, Taiwan was studied according to two-stage analytical process applied (NDVI image and Maximum Likelihood Classification) on Landsat, SPOT and QuickBird imagery (Lee and Yeh, 2009). Besides, Upanoi and Tripathi (2003) also proposed a fast and easy classification by compute RGB-NDVI image from multi-dates satellite data (Landsat-5 TM and Landsat-7 ETM+ data) follow by ISODATA unsupervised classification to monitor the changes of mangrove forest in Krabi, Thailand.

The objective of this study was to quantify the former and current mangrove forest distribution around Penang Islands using THEOS and Landsat-7 ETM+ satellite data.

## MATERIALS AND METHODS

**Study area:** Penang Island is located within latitudes 5°12-5°30'N and longitudes 100°09-100°26' E (Fig. 1).


Fig. 1: Location of the study area

Penang state comprises of two parts, the small island of Penang (known as Penang Island) and a coastal strip on the mainland (known as Province Wellesley). The island and mainland are linked by a 13.5 km long Penang Bridge and ferry services. Total population in Penang is estimated to be around 1,577,300 people with annual population of 2.0%.

Penang has an equatorial climate which is consist of warm and sunny days throughout the entire year due to its proximity to the equator line. The mean daytime and night time temperature is between 27-30°C and 22-24°C, respectively with annual temperature range from 23- 32°C. The humidity is relatively high (70%-90%) with mean annual rainfall of 267 cm (Ahmad *et al*., 2006). Penang Island is virtually free from major natural disasters which can cause life loss or death such as volcanic disruption, tornados, hurricanes and earthquakes.

Fig. 2: Landsat raw satellite data

Fig. 3: THEOS raw satellite data

**Sources of imagery:** Two satellite images were used in this study. One is the Landsat 7 ETM+data acquired on 17 Jan 2002 and another one is the THEOS data obtained on 29 January 2010. The two satellite data have panchromatic and multi-spectral band sensor in specific wavelength. Landsat and THEOS sensor consist of one panchromatic band but there are seven multi-spectral bands for Landsat and four multi-spectral bands for THEOS. The resolution of multi-spectral bands for Landsat is 30 m and 15 m for THEOS sensor. Landsat data contained in path 128, row 56 which have 7 multi-spectral bands (blue, green, red, infrared, two short-wave infrared and thermal) has been downloaded from United State Geological Survey Global Visualization Viewer (USGS GloVis). THEOS data which have 4 multi-spectral bands (blue, green, red and infrared) has been obtained form Geo-Informatics and Space Technology Development Agency (GISTDA). The two satellite data were chosen due to the fact that the 2 images have <10% cloud coverage and almost cloud-free over the study site (Sun *et al*., 2009). As Penang Island is located in equatorial region, it's very hard to obtain a totally cloud-free satellite imagery. The raw data for Landsat and THEOS satellite imagery for Penang Island were shown in Fig. 2 and 3.

**Image pre-processing:** The multi-temporal images used must have same coordinate system, projection and resolution in order to detect changes in land cover (Chen *et al*., 2006). Pixel based analysis will be used in this change detection monitoring. Radiometric and atmospheric correction was carried out on the Landsat and THEOS data to remove the non-uniformities on the imaging system and atmospheric effects. THEOS image was resampled to 30 meters resolution by using nearest neighbor method with the aid of PCI Geomatica version 10.3.2 image processing software. After resampling process, geometric correction was carried out to co-register the coordinate of Landsat into THEOS data. Twenty points in the study site were used as Ground Control Point (GCP) collection with Landsat image as geocoded image to correct the coordinate of THEOS data. Root Mean-square Error (RMSE) serve as a good indicator to detect the accuracy of the co-registered images and RMSE value of <0.5 pixels is considered good accuracy (Lunetta and Elvidge, 1999). A value of more than 1 pixels will leads to misinterpretation of land cover at same point in the two images. Overall RMSE value attained in this study is less than 0.5 pixels. The ratio of Near-infrared (NIR) reflectance over visible reflectance was used to detect the existence of cloudy pixel over study area in cloud masking process as shown in equation below (Saunders and Kriebel, 1988):

$$Q = R_2/R_1 \tag{1}$$

where, Q is the ratio of NIR reflectance to visible reflectance, $R_2$ is the NIR reflectance and $R_1$ is the visible reflectance.

**Image classification:** The intent of this step is to categorize all of the pixels in the image scene into several land cover classes based in their pixel value. This categorized data can then be used to produce thematic maps of the land cover present in the image. After the two images had filtered through 3×3 low pass filters, supervised classification was chosen to classify the entire image as we may know what are the features on the image represent. The two images were processed using Geomatica version 10.3.2 software package. In supervised classification, we select the recognized regions within an image (pixels) based on ground truthing such as field visit to the site or visual interpretation of the already known area to create a sample area called training sites. Multiple vector layers consist of polygons which are chosen as training sites are then digitized into the raster scene. This training site is utilized to train the software has enough information to create the spectral signatures of the entire image. These signatures will then be used to classify all the unknown pixels in the entire scene.

Maximum Likelihood Classifier (MLC) was performed instead of minimum distance-to-mean and parallelepiped classifier due to the fact that MLC is superior and always has the highest accuracy among the three classifiers as proven by researchers before. In MLC technique, it classifies an unknown pixel for each land cover class base on the probability that it belonging to that class. If the probability values fail to determine its most likely class in any of the class, the corresponding pixel will be classified as an unknown region. In MLC, pixels are assigned to a category/classes based on highest probability. Hence, when different land cover classes have very similar spectral characteristic with each other, the difficulty of Maximum Likelihood classifier to distinguish the pixels may lead to 'salt and pepper' effects in final classification map (Mustapha *et al.*, 2010).

In this study, 2 sets of different sensor satellite imagery THEOS and Landsat data which had been projected to same resolution was classified into 5 classes using MLC supervised classification. A total of 100 training samples (20 samples for each class) were selected and used in the classification process. For THEOS and Landsat scene, all of the four bands and seven bands were used in the classification analysis.

**Accuracy verification:** Post-classification analysis (accuracy assessment) was tested on the classified land cover map to express the degree of correctness of the classification. Agreement between the classified data and reference data was tested by using 500 randomly sample points distributed around the entire image scene. Same random points were applied into the two classified image.

Error (confusion) matrix was generated to compare the reliability of the classified and reference data. Major diagonal in the matrix reveals the total number of pixels which had been correctly classified and other non-diagonal elements in the matrix resemble the omission and commission error (Congalton, 1991). Omission error is represented by non-diagonal column elements and commission error is represented by non-diagonal row elements. Producer's accuracy, user's accuracy, overall accuracy and kappa coefficient for each land cover class will be evaluated from the confusion matrix results. Producer's accuracy is calculated by dividing the number of correctly classified pixels in each class by the total number of reference pixels in that class (the column total). User's accuracy is calculated by dividing the number of correctly classified pixels in each class by the total number of classified pixels in that class (the row total). Overall accuracy is calculated by dividing the total number of correctly classified pixels (the sum of all elements along the major diagonal) by the total number of reference pixels (Lillesand and Kiefer, 1994).

Kappa coefficient is a statistical measurement of the agreement between two maps (classified map and reference map) and indicates how each classification differ from a random classification of the class types. It is computed by takes into account the whole error matrix instead of only the diagonal elements and incorporated the non-diagonal elements as a product of row and column marginal totals in the analysis. Computation of kappa coefficient (K) is given in equation (Bishop *et al.*, 1975):

$$K = \frac{N\sum_{i=1}^{r} X_{ii} - \sum_{i=1}^{r} X_{i+}.X_{+i}}{N^2 - \sum_{i=1}^{r} X_{i+}.X_{+i}} \tag{2}$$

where, r is number of rows in confusion matrix, $x_{ii}$ is number of observation in row i and column i (the major diagonal in confusion matrix), $x_{i+}$ and $x_{+i}$ are marginal totals of row i and column i, respectively and N is number of observation.

## RESULTS

The thematic maps produced from the supervised maximum likelihood classification were showed in Fig. 4 and 5. Figure 4 and 5 are the classification results computed from 2002 Lansat-7 ETM+ and 2010 THEOS data, respectively. In this study, the land cover is divided into five main classes consist of forest and grassland, mangrove, urban land, bare soil and water. From the visual interpretation of map produced, we can observe clearly that mangrove plants or trees are commonly concentrated on the mudflats along west coastal region. The area cover with mangrove in year 2002 is about 6.34 square kilometers (1.14%) from Table 1. Whereas in year 2010 the mangrove cover was increased to 7.12 square kilometers (1.28%). Table 1 below show the statistical analysis on the land cover changes detection between 2002 and 2010. The area of mangrove changes from 2002-2010 is approximately 0.78 square kilometers with corresponding percentage changes of 12.30%. For other non-mangrove vegetation (other four classes), forest and grassland, water, urban and bare soil cover an area of 175.85, 242.64, 76.08, 55.23 $km^2$ in year 2002 and 190.03, 250.82, 77.47, 30.70 $km^2$ in year 2010, respectively.

Between 8 years periods, the obvious changes of areas is among the bare soil category with negative change of 44.41%. In other words, bare soil area was declined around 5.55% per year. On the contrary, urban land only have insignificant changes of 1.83% in area. For water, the area changes is approximately 3.37% and the changes in forest and grassland is about 8.06%. Confusion (error) matrix for the different land cover was shown in Table 2 and 3 to test the reliability and accuracy of the maximum likelihood classification mapping result. Error matrix consisted of square array of rows and columns with each row and column represent one land cover in the classification.

Based on Table 2, the classification of mangrove vegetation is being classified correctly in the classified data with user's and producer's accuracy of 100%. From Table 3, the user's accuracy for mangrove was decreased to 77.78%. The producer's and user's accuracies for all the other land cover class is quite high (>70%) except for the user's accuracy for bare soil category (63.46%). Producer's accuracy measure how well a specific land area has been classified and informs us about the proportion of correctly labelled object in the reference data whereas

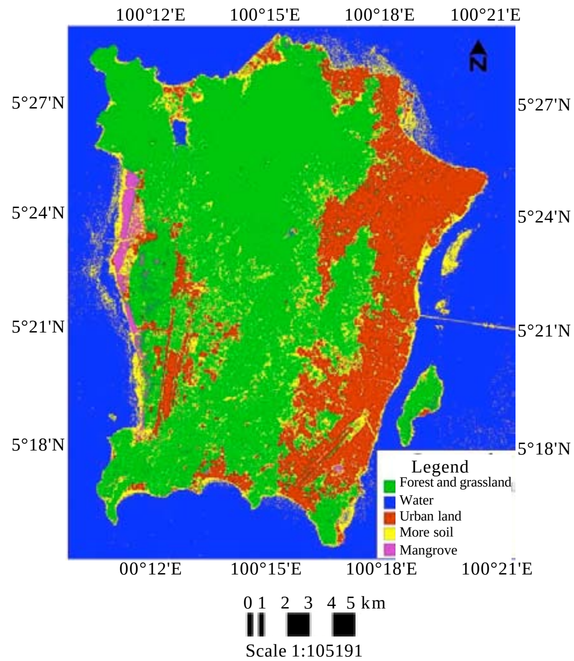


Fig. 4: Classification map for landsat data

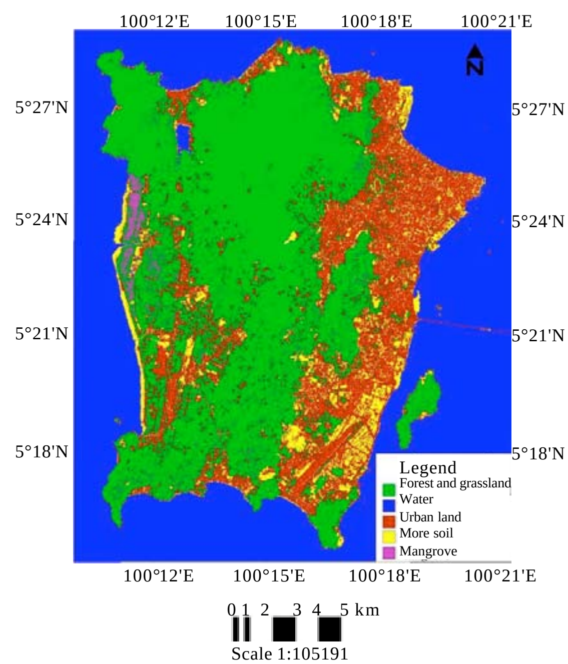


Fig. 5: Classification map for THEOS data

user's accuracy measures the reliability of the generated classified map and indicates the probability that a specifically classified object also belongs to that specific class in reality. The user's accuracies for Landsat data for each category of class were as follows: 98.72% for forest

Table 1: Statistical analysis of the land cover changes from 2002-2010

| | 2002 Landsat map | | 2010 THEOS map | | Change in area (2002-2010) | |
|---|---|---|---|---|---|---|
| Class name | Area cover (km$^2$) | Image (%) | Area cover (km$^2$) | Image (%) | km$^2$ | % |
| Forest and grassland | 175.85 | 31.62 | 190.03 | 34.17 | 14.18 | 8.06 |
| Water | 242.64 | 43.63 | 250.82 | 45.10 | 8.18 | 3.37 |
| Urban land | 76.08 | 13.68 | 77.47 | 13.93 | 1.39 | 1.83 |
| Bare soil | 55.23 | 9.93 | 30.70 | 5.52 | -24.53 | -44.41 |
| Mangrove | 6.34 | 1.14 | 7.12 | 1.28 | 0.78 | 12.30 |
| Total | 556.14 | 100.00 | 556.14 | 100.00 | | |

Table 2: Error (confusion) matrix of Landsat 2002 map

| | Reference data | | | | | | |
|---|---|---|---|---|---|---|---|
| Classified data | Forest and grassland | Water | Urban land | Bare soil | Mangrove | Total | UA (%) |
| Forest and grassland | 154.00 | 0.00 | 1.00 | 1.00 | 0 | 156 | 98.72 |
| Water | 0.00 | 206.00 | 0.00 | 0.00 | 0 | 206 | 100.00 |
| Urban land | 2.00 | 0.00 | 74.00 | 7.00 | 0 | 83 | 89.16 |
| Bare soil | 6.00 | 2.00 | 11.00 | 33.00 | 0 | 52 | 63.46 |
| Mangrove | 0.00 | 0.00 | 0.00 | 0.00 | 3 | 3 | 100.00 |
| Total | 162.00 | 208.00 | 86.00 | 41.00 | 3 | 500 | |
| PA (%) | 95.06 | 99.04 | 86.05 | 80.49 | 100 | | |

PA: Producer's accuracy, UA: User's accuracy

Table 3: Error (confusion) matrix of THEOS 2010 map

| | Reference data | | | | | | |
|---|---|---|---|---|---|---|---|
| Classified data | Forest and grassland | Water | Urban land | Bare soil | Mangrove | Total | UA (%) |
| Forest and grassland | 163.00 | 0.00 | 5.00 | 1.00 | 0 | 169 | 96.45 |
| Water | 0.00 | 209.00 | 0.00 | 2.00 | 0 | 211 | 99.05 |
| Urban land | 6.00 | 1.00 | 73.00 | 4.00 | 0 | 84 | 86.91 |
| Bare soil | 0.00 | 0.00 | 7.00 | 20.00 | 0 | 27 | 74.07 |
| Mangrove | 2.00 | 0.00 | 0.00 | 0.00 | 7 | 9 | 77.78 |
| Total | 171.00 | 210.00 | 85.00 | 27.00 | 7 | 500 | |
| PA (%) | 95.32 | 99.52 | 85.88 | 74.07 | 100 | | |

PA: Producer's accuracy, UA: User's accuracy

Table 4: Accuracy assessment results for Landsat and THEOS map

| Results | Landsat | THEOS |
|---|---|---|
| Overall accuracy (%) | 94.000 | 94.400 |
| Kappa statistic | 0.913 | 0.917 |

and grassland, 100.00% for water, 89.16% for urban land and 63.46% for bare soil. In THEOS data, the user's accuracies were 96.45% for forest and grassland, 99.05% for water, 86.91% for urban land and 74.07% for bare soil. The overall accuracy and kappa coefficients were evaluated from error matrix in Table 4.

The overall accuracy obtained from Landsat and THEOS data by maximum likelihood classification were 94.00 and 94.40%, respectively. The high kappa statistic (coefficient) of 0.913 and 0.917 also achieved as well and these results indicate that the two maps produced from classical supervised classification have very good reliability and accuracy.

## DISCUSSION

Through the results and analysis on monitoring of mangrove changes occurs from 2002 to 2010, the increase in mangrove area (reforestation) from the study site (6.34-7.12 km$^2$) may be due to the conservation and reforestation efforts done by the state government. In the latest Star news on 27 April 2010, Penang State Government has organised a mangrove project at the Gurney Drive to plant 1,000 mangrove saplings at the seafront of Marina Bay condominiums near Tanjung Tokong. It was one part of the long-term effort done by state government in order to achieve the target to have 26 million mangrove trees by 2014. However, 54, 000 mangrove trees also were planted in Penang state in year 2009 results from the hard work cooperation of state government along with the concerned residents. Hence, the reforestation of the mangrove cover is reasonable.

The declined in bare soil region (55.23-30.70 km$^2$) at the western, eastern and northern parts of the study area may due to the change of tidal conditions at the time of data acquisition. Despite this, decrease of bare soils in coastal areas, the areas of bare soils increased due to the change in the southeastern part (i.e., changes of urban areas in 2002 into bare soils in 2010). This phenomenon occurs probably due to the corner reflectance of factory site at that area which cause the pixel to be different from the normal urban area's pixel. The slight increase in urban area (13.68-13.93%) is due to high demands of development into residential and industrial area to compensate for the increasing population in Penang. The forest and grassland region in western part rises (31.62-34.17%) owing to the misclassify pixels of mangrove area into forest and grassland.

The decrease of user's accuracy in the mangrove category (100-77.78%) is mainly due to the commission error of 2 pixels improper included in the mangrove category. As the 2 pixels is originally belongs to forest and grassland category, because of the almost same spectral signature between forest and grassland with mangrove vegetation, the wrong classified pixels is somehow predictable. As stated by Cracknell (1998), mixed pixels usually have been recognized as a main problem that will influence the accuracy of remotely sensed data in land use/cover classification. Indeed, the poor user's and producer's accuracies in bare soil and urban land are also expected. This is due to the fact that the urban areas (mainly factory area) have very similar spectral with bare soil. This kind of misleading in pixels (spectral) will cause misclassified pixels between these 2 classes and hard to distinguish.

The study of mangrove in Penang Island is limited although there was some research on mangrove had been done in Malaysia. By monitor the mangrove changes over Penang Island, the developer can easily identify the mangrove area in a country and prevent the deforestation of mangrove when carrying out land planning. With this kind of mangrove mapping data, government can use the data as database to monitor and protect the unique mangrove ecosystem for our future generation. In future study, in order to have deeper knowledge and biophysical properties on mangrove ecosystem, species of mangrove need to be studied and identified.

## CONCLUSION

In this study, the monitoring of the mangrove cover in Penang Island was performed using Landsat and THEOS data. The former and current conditions in mangrove cover were investigated. High accuracy in kappa coefficients were obtained from the error matrix of both set data by using maximum likelihood classification algorithm. In general, the high resolution of THEOS satellite imagery can be used effectively along with the Landsat data to separate the mangrove cover from vegetation area and further it can be utilized for multi-date monitoring purpose. Further research can be carried out to discriminate the mangrove species in Penang Island by examine theirs spectral reflectance properties in detail.

## ACKNOWLEDGMENTS

The authors gratefully acknowledge the financial support from the short term Research University Postgraduate Research Grant Scheme (USM-RU-PGRS), account number: 1001/PFIZIK/843094 and USM fellowship used to carry out this project. We would like to thanks the technical staff who involved in this project. Thanks are also extended to USM for support and encouragement.

## REFERENCES

Ahmad, F., A.S. Yahay and M.A. Farooqi, 2006. Characterization and geotechnical properties of penang residual soils with emphasis on landslides. Am. J. Environ. Sci., 2: 121-128.

Bishop, Y.M.M., S.E. Fienberg and P.W. Holland, 1975. Discrete Multivariate Analysis. 2nd Edn., MIT Press, Cambridge, MA., ISBN: 0262021137, pp: 557.

Chen, X.L., H.M. Zhao, P.X. Li and Z.Y. Yin, 2006. Remote sensing image based analysis of the relationship between urban heat island and land use/cover changes. Remote Sens. Environ., 104: 133-146.

Congalton, R.G., 1991. A review of assessing the accuracy of classifications of remotely sensed data. Remote Sens. Environ., 37: 35-46.

Coulibaly, L. and K. Goita, 2006. Evaluation of the potential of various spectral indices and textural features derived from satellite images for surficial deposits mapping. Int. J. Remote Sens., 27: 4567-4584.

Cracknell, A.P., 1998. Synergy in remote sensing-what's in a pixel. Int. J. Remote Sens., 19: 2025-2047.

Emch, M. and M. Peterson, 2006. Mangrove forest cover change in the Bangladesh *Sundarbans* from 1989-2000: A remote sensing approach. Geocarto Int., 21: 5-12.

Gong, W.K. and J.E. Ong, 1990. Plant biomass and nutrient flux in a manager mangrove forest in Malaysia. Estuarine, Coastal Shelf Sci., 31: 519-530.

Green, E.P., C.D. Clark, P.J. Mumby, A.I. Edwards and A.C. Ellis, 1998. Remote sensing techniques for mangrove mapping. Int. J. Remote Sens., 19: 935-956.

Green, E.P., P.J. Mumby, A.J. Edward and C.D. Clarks, 1996. A review of remote sensing for the assessment and management of tropical coastal resources. Coastal Manage., 24: 1-40.

Ibrahim, K., R.Z. Bukhari, K. Jusoff and M.H. Ismail, 2010. Atmospheric based correction vegetation index for mangrove mapping at Kelantan Delta. Proceedings World Engineering Congress, August 2-5, 2010, Kuching, Sarawak, Malaysia, pp: 1-9.

Jensen, R., P. Mausel, N. Dias, R. Gonser, C. Yang, J. Everitt and R. Fletcher, 2007. Spectral analysis of coastal vegetation and land cover using AISA+ hyperspectral data. Geocarto Int., 22: 17-28.

Lee, T.M. and H.C. Yeh, 2009. Applying remote sensing techniques to monitor shifting wetland vegetation: A case study of Danshui River estuary mangrove communities, Taiwan. Ecol. Eng., 35: 487-496.

Lillesand, T.M. and R.W. Kiefer, 1994. Classification Accuracy Assessment. In: Remote Sensing and Image Interpretation, Lillesand, T. and R.W. Kiefer (Eds.). 3rd Edn. John Wiley and Sons Inc., New York, USA., pp: 612-618.

Liu, Z.G., J. Li, B.L. Lim, C.Y. Seng and S. Inbaraj, 2007. Object-based classification for mangrove with VHR remotely sensed image. Proceedings of the International Conference on Geoinformatics 2007: Remotely Sensed Data and Information, May 25-27, 2007, Nanjing, China.

Lunetta, R.S. and D.E. Elvidge, 1999. Remote Sensing Change Detection: Environmental Monitoring Methods and Applications. Taylor and Francis/CRC Press, London, UK., ISBN-13: 9780748408610, Pages: 318.

Mitsch, W.J., J.C. Lefeuvre and V. Bouchard, 2002. Ecological engineering applied to river and wetland restoration. Ecol. Eng., 18: 529-541.

Mustapha, M.R., H.S. Lim and M.Z. Mat Jafri 2010. Comparison of neural network and maximum likelihood approaches in image classification. J. Applied Sci., 10: 2847-2854.

Polpanich, O., W.C. Shing, J.A. Collin, M.A. Talib and L. Samarakoon, 2009. Mangrove conversion and aquaculture development in Sabah, Malaysia: Remote sensing and GIS-based approach for assessing land use change in mangroves. Proceeding of the 30th Asian Conference on Remote Sensing, October 18-23, 2009, Beijing, China, pp: 1-6.

Saunders, R.W. and K.T. Kriebel, 1988. An improved method for detecting clear sky and cloudy radiances from AVHRR data. Int. J. Remote Sens., 9: 123-150.

Sulong, I., H. Lokman, K. Tarmizi and A. Ismail, 2002. Mangrove mapping using landsat imagery and aerial photography: Kemaman district, Terengganu, Malaysia. Environ. Dev. Sustain., 4: 135-152.

Sun, Z., R. Ma and Y. Wang, 2009. Using landsat data to determine land use changes in Datong basin, China. J. Environ. Geol., 57: 1825-1837.

Tan, K.C., H.S. Lim, M.Z. MatJafri and K. Abdullah, 2010. Landsat data to evaluate urban expansion and determine land use/land cover changes in Penang Island, Malaysia. Environ. Earth Sci., 60: 1509-1521.

Upanoi, T. and N.K. Tripathi, 2003. A satellite based monitoring of changes in mangroves in Krabi, Thailand. Proceedings of the Map Asia Conference, October 13-15, 2003, Kuala Lumpur, Malaysia, pp: 1-10.